EVALUATION OF 10V CHIP POLYMER TANTALUM CAPACITORS FOR SPACE APPLICATIONS

Alexander Teverovsky

ASRC Federal, NASA/GSFC Code 562, Greenbelt, MD 20771, USA

Alexander.A.Teverovsky@nasa.gov

CONTENTS

INTRODUCTION

Replacement of manganese oxide as a cathode material in chip tantalum capacitors by conductive polymers allows for higher operating frequencies, lesser equivalent series resistances (ESR) and a lower power dissipation in the parts. Another benefit of chip polymer tantalum capacitors (CPTCs) is a relatively safe failure mode. Contrary to MnO2 capacitors that often fail with ignition causing damage to the whole system, failures in polymer capacitors are much less dramatic. In order to prevent surge current failures that are specific to MnO2 capacitors, operation voltages should be de-rated. Due to different mechanisms of failure, manufacturers are suggesting much less voltage derating for polymer (80% to 90% of the rated voltage, VR) compared to the MnO2 capacitors (typically 50% derating is used), which is yet another benefit of CPTCs [1-3].

A better performance and improved quality of polymer capacitors that had been achieved over the last years made these parts preferred components for many commercial applications, and currently, majority of new tantalum capacitors have been produced with polymer cathodes. CPTCs have been developed first for commercial applications, but now they are used in reliability-demanding automotive (e.g. T591/T598 series from KEMET, TCQ series from AVX), medical, military and space systems. Due to catastrophic failures of MnO2 capacitors and acceptable results of testing of polymer capacitors, Raytheon is using CPTCs in some airborne applications from 2012 [4]. DLA L&M issued drawings #04051 and #04052 for CPTCs in 2006 and updated them in 2013.

The first polymer capacitors (late 1990's) were manufactured using in-situ polymerization of poly(3,4-ethylenedioxythiophene (PEDOT) by chemical reactions between the oxidizer and monomer [5]. Polymerization occurs by the oxidation of 3,4-ethylenedioxythiophene (EDOT) with catalytic iron (III) sulfate compositions [6]. First CPTCs had large leakage currents and small breakdown voltages (VBR) thus limiting the operating range to below 10 V. A significant increase in VBR and reduction of DC Leakage (DCL) had been achieved by employment of a pre-polymerized PEDOT/PSS (polystyrene sulfonate) suspensions. Implementation of new conductive polymers in 2009 allowed for manufacturing of high-voltage capacitors with low leakage currents [7]. Currently, AVX and KEMET, are in the process of developing high-voltage (up to 125 V) polymer capacitors that can operate at high temperatures (above 125 °C) [7, 8].

Although the size of particles in slurries of the pre-polymerized PEDOT/PSS is low, ~ 30 nm [6], it is still too large to penetrate into the pellet of high-CV value capacitors and assure full surface coverage of the Ta2O5 dielectric. For this reason, the majority of capacitors rated to 10 V and less are manufactured using in-situ polymerization process. In many cases a combination of the in-situ polymerization and pre-polymerized polymers, so called hybrid technology, is used. According to this technology, first layers during cathode formation are made using in-situ PEDOT and then pre-polymerized PEDO/PSS compositions are applied [9].

The mechanism causing increased leakage currents in capacitors using in-situ polymerization is not fully understood and requires additional analysis. One of the reasons for high DCL might be insufficient self-healing in polymer compared to MnO2 capacitors [10]. Although polymer capacitors do have the ability to self-heal, their high conductivity means less localized heating at the defect site. As a result, the self-healing is less effective, and for this reason some defects are not healed completely causing higher leakage currents. Y. Freeman et al. [11], suggested that high DCL is due to formation of defects and oxygen vacancies in the Ta2O5 film near the Ta2O5/PEDOT interface as a result of the in-situ polymerization. Possible changes in the surface charge at the Ta2O5-polymer interface that were attributed to residuals of the in-situ polymerization reaction might be also a factor affecting leakage currents [9].

Life testing of MnO2 capacitors showed that these parts are mostly prone to infant mortality (IM) failures, which justifies using so-called Weibull grading test (WGT) as a major screening and qualification procedure [12]. However, CPTCs are more likely to fail due to wear-out processes, thus making WGT not applicable. For this reason, a new reliability assessment strategy has been developed by KEMET [13]. This new Failure Rate (FR) assessment process includes reflow-mounting of disposable samples and testing under accelerated conditions to validate the target failure rate. Sample size, accelerated test conditions, test duration, and failure criteria are chosen to match the specific part type using equations based on the wear-out mechanism. Unfortunately, this approach does not prevent possible IM or random failures, requires selection of adequate failure criteria, and assessment of the reliability acceleration factors.

CPTCs have a limited operational temperature range compared to MnO2 capacitors and can degrade substantially under environmental stresses, in particular, during long-term exposure to high temperatures (above ~100 °C) and under combined stresses of temperature and humidity [8]. Testing at 85% RH/85 °C and at temperatures exceeding 105 °C can result in increasing leakage currents, ESR and dissipation factors [5, 14, 15].

Studies [8, 16] have shown that a certain amount of moisture is essential for normal operation of polymer capacitors. For this reason, polymer hermetically sealed (PHS) tantalum capacitors that have been manufactured for harsh military and space applications have some moisture added to the case before sealing. Our studies [17] confirmed an important role of moisture in high-voltage PHS capacitors. No degradation of capacitance or ESR was observed during 1000 hour storage testing at 150 °C, whereas this testing resulted in a substantial degradation of capacitance (decrease to below 40% of the initial value) and ESR (increase up to 10 times) for the parts that are not sealed.

If presence of moisture is necessary for normal operation of CPTCs, degradation might be expected when moisture is released from polymers in vacuum. Moisture desorption occurs also during high temperature storage (HTS) testing in air. Variation of characteristics of CPTCs during HTS might be due also to thermal oxidative processes in polymers. For this reason, the effect of vacuum cannot be simulated by HTS and should be investigated by testing in vacuum.

Conditions that can cause CPTCs to dry out, such as operation in vacuum or during reflow soldering, may cause capacitors to exhibit an anomalous charging behavior [2, 8]. This behavior might increase substantially the amount of time and energy necessary to charge the capacitors, and requires additional investigation. Anomalous relaxation of leakage currents in dry capacitors is likely specific for CPTCs using PEDOT/PSS polymers, and was not observed in capacitors with in-situ polymerization [8, 9]. This indicates a need for a separate analysis of degradation processes in low-voltage capacitors that employ mostly in-situ polymerized PEDOT and high-voltage capacitors that use pre-polymerized PEDOT/PSS polymers.

Until recently, it was considered that although some polymer capacitors can be rated to 125 °C, most are limited to 85 °C or 105 °C applications, and given the limitation of the material, it appeared unlikely this upper limit will be increased significantly in the near future [10]. However, in 2014 KEMET and AVX introduced automotive grade capacitors that

can pass biased testing at 85 °C/85% RH for 1000 hours and unbiased HTS at 125 °C for 1000 hours. This had been achieved primarily by improving the packaging system [5] that slows or prevents air or moisture from reaching conductive polymer layers. AVX has introduced TCQ series of AEC-Q200 compliant CPTCs. To meet the requirements of automotive industry, specific enhancements in design, polymerization process and additional humidity protection coats have been incorporated [3].

Available data indicate that environmental stresses might have a more profound effect on CPTCs compared to MnO2 capacitors; however, specifics of the degradation processes have not been studied sufficiently. More testing and analysis are necessary to understand mechanisms of the degradation and develop adequate screening and qualification procedures to assure reliable applications of CPTCs in space systems. Because different polymers are used for low-voltage and high-voltage capacitors, their reaction to environmental stresses might be different. This requires a separate analysis of environmental stresses for low-voltage and high-voltage capacitors.

In this work, a comparative analysis of performance and degradation in low-voltage polymer and MnO2 capacitors under vacuum and air storage conditions has been carried out. Leakage currents in CPTCs have been studied in a wide range of temperatures and voltages. Highly Accelerated Life Testing (HALT) in the range from 85 ºC to 145 ºC has been carried out to assess the temperature and voltage acceleration factors of degradation. Different lots of general purpose and automotive grade capacitors have been used to reveal common trends during HALT and HTS testing. Mechanisms of degradation and failures, and requirements for screening and qualification testing are discussed.

PART TYPES

Types of CPTCs used in this study, their intended applications, lot date codes or year of manufacturing, and specified characteristics are shown in Table 1. The limit for leakage currents is calculated as $DCL_{max} = 0.1CV$, where DCL is in μA, C in μF, and V is in volts. All parts were manufactured by KEMET and rated to 10 V. Groups from 5 to 20 samples from each lot were typically used for environmental testing.

Capacitance and dissipation factors were tested at 120 Hz and ESR at 100 kHz using Hewlett-Packard 4274A LCR meter and Agilent 4294A impedance analyzer. The specified values of ESR for T530 series were substantially (~4 times) less than for other part types because these parts employed multi-anode construction.

Variations of leakage currents with time were monitored using a PC-based system and Agilent scanners that measured voltage drop across resistors connected in series with each capacitor. Typically, leakage currents were monitored for 20 min under polarization voltage and 20 min at 0 V applied immediately after polarization. Examples of *I-t* characteristics are shown in Fig 1.

Table 1. Part types used in this study.

PN	application	LDC	C, μF	DF_{max}, %	ESR_{max}, mohm	DCL_{max}, uA	Temp. Range
T530X337M010AHE010	general	DC1225	330	8	10	330	-55C to +125C
T530D227M010AHE010	general	DC1316	220	8	10	220	-55C to +125C
T530D157M010AHE006	general	DC1347	150	8	6	150	-55C to +125C
T598D227M010ATE040	auto	(2015)	220	10	40	220	-55C to +125C
T525B336M010ATE080	auto, ind., MIL	(2011)	33	10	80	33	-55C to +125C
T520A106M010ATE080	general	(2011)	10	10	80	10	-55C to +105C
T520B336M010ATE070	general	(2011)	33	10	70	33	-55C to +105C
T525D227M010ATE025	auto, ind., MIL	(2011)	220	10	25	220	-55C to +125C
T520D227M010ATE018	general	(2011)	220	10	18	220	-55C to +105C

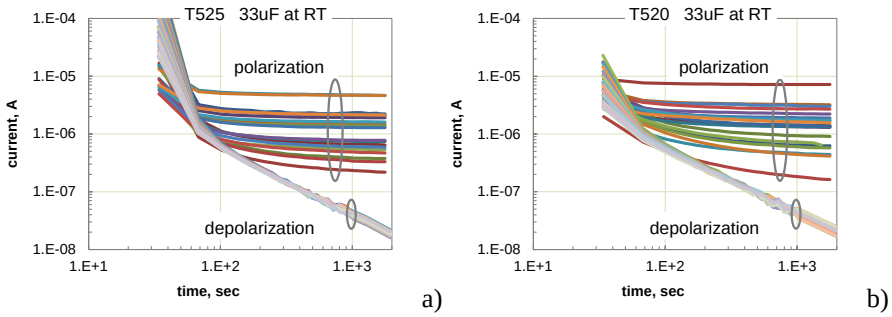

Fig. 1. Typical current relaxation during polarization and depolarization for 33 µF 10 V capacitors. (a) T525 series; (b) T520 series.

LEAKAGE CURRENTS

Absorption and Intrinsic Currents

Typically, absorption currents that are decreasing with time according to a power law, $I \sim t^{-n}$, where n is a constant close to one, prevail at room temperature in tantalum capacitors [18]. Intrinsic leakage currents caused by conduction of the dielectric prevail at high temperatures or voltages. However, it is not so for low-voltage CPTCs. For these parts depolarization currents similar to MnO2 capacitors decrease with the exponent n = 1 ±0.1; however, their amplitude is substantially less than for polarization currents.

For CPTCs intrinsic currents are prevailing after 300 sec of polarization even at room temperatures, RT, (see Fig. 2). Analysis shows that polarization currents exceed depolarization currents measured after 300 sec from 50 to 200 times.

Depolarization or absorption currents, I_{abs}, in low-voltage CPTCs similar to MnO2 or wet tantalum capacitors depend mostly on the value of capacitance and increase linearly with voltage (up to ~ 1.2VR). This feature is common for absorption processes in tantalum and ceramic capacitors [18, 19]. Typically, I_{abs} have a weak temperature dependence. However, in low-voltage CPTCs absorption currents increase with temperature by ~4 times from 22 ºC to 145 ºC suggesting an increased concentration of deep electron traps at the polymer/Ta2O5 interface. Analysis shows that leakage currents in low-voltage CPTCs even at room temperature and rated voltages are controlled by the intrinsic conduction processes in the Ta2O5 dielectric.

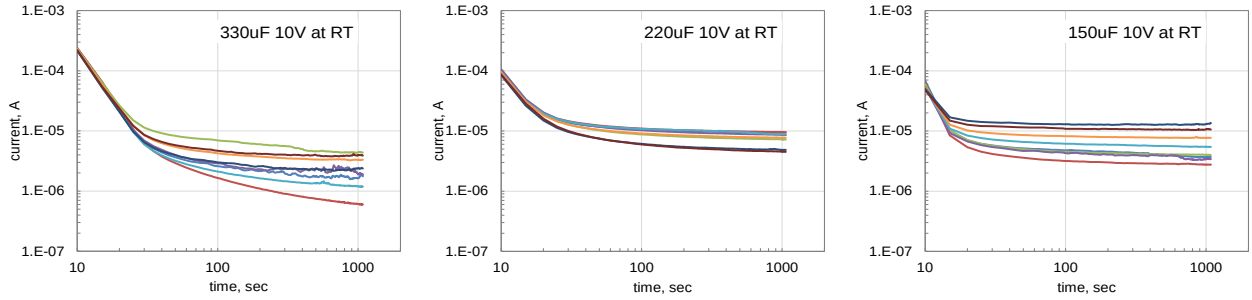

a) b) c)

Fig. 2. Relaxation of leakage currents in T530 CPTCs at room temperature.

Effect of Voltage

Leakage currents were measured with respect to time at voltages ranging from 2.5 V to 13 V and temperatures from room to 145 ºC. To ensure that absorption processes did not affect the measurements, steady state currents that correspond to intrinsic conduction of the dielectric were measured after 1000 sec of electrification. Typical variations of leakage currents with electric field in Schottky coordinates for samples of T520 and T525 capacitors are shown in Fig. 3. For calculations of the electric field, the thickness of the dielectric for 10 V capacitors was assumed 55 nm. *I(E)* characteristics on each chart are plotted for two samples, one with minimal and one with maximal current in the group. Fig. 3c shows variations of the median leakage currents measured at different temperatures with electric field for T520 220 µF capacitors. The slope of lines, α, reduces from 6.1E-4 $(m/V)^{0.5}$ at room temperature to 4.7E-4 $(m/V)^{0.5}$ at 145 ºC. In all cases, experimental data can be accurately enough approximated with straight lines with slopes slightly decreasing with temperature.

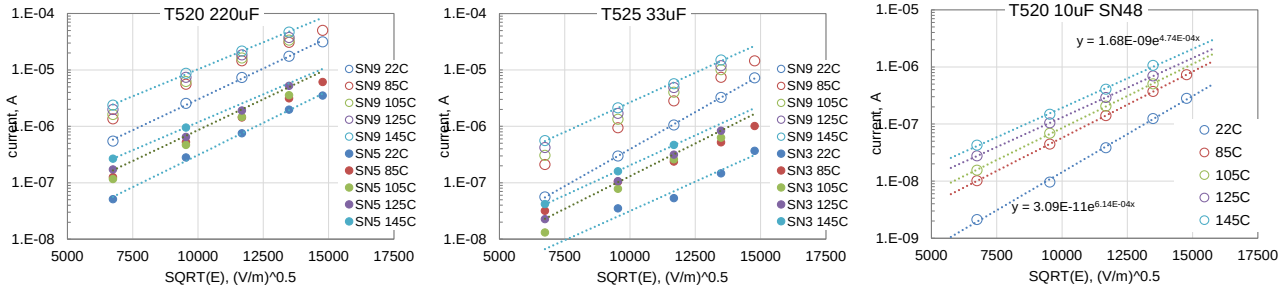

a) b) c)

Fig. 3. Variations of leakage currents with electric field for T520 220 µF (a), T525 33 µF (b), and T520 10 µF (c) capacitors at differrent temperatures and voltages varying from 2.5 V to 12 V. Solid and empty marks in Fig. (a, b)

correspond to samples with maximal and minimal currents in each group. Marks in Fig. (c) correspond to the median values of currents.

Similar *I(E)* characteristics in T520/T525 capacitors were measured after HALT at 125 ºC, 12 V for 100 hours. As it will be shown below, HALT resulted in a substantial degradation of leakage currents. However, samples with leakage currents increased almost two orders of magnitude had slopes α in a relatively narrow range, from 4.6E-4 $(m/V)^{0.5}$ to 5.3E-4 $(m/V)^{0.5}$, which is close to the initial data.

Temperature variations of the slopes measured for different samples of type T520/T525 capacitors are shown in Fig. 4. The chart shows also data calculated based on the Schottky model. According to the model, the current is an exponential function of temperature and electric field:

$$I \sim \exp\left(-\frac{U}{kT}\right), \qquad U = \Phi_B - \beta_S E^{1/2}, \qquad \beta_S = \left(\frac{q^3}{4\pi\varepsilon_0\varepsilon}\right)^{1/2} \tag{1}$$

here Φ_B is the barrier height, β_s is the Schottky constant, k is the Boltzmann constant, q is the electron's charge, ε_0 is the dielectric constant in vacuum, T is the absolute temperature, and ε is the high-frequency dielectric constant of the dielectric.

It should be noted that Schottky model is not applicable to the metal-dielectric systems that have a mean free path of electrons less than the thickness of the dielectric. Simmons [20] have modified Schottky model for solid dielectrics, but in the modified form the dependence of the barrier height on the electric field remains the same.

Eq.(1) can be presented in a form:

$$\ln(I) = A - \frac{\Phi_{B.}}{kT} + \frac{\beta_S}{kT} E^{1/2} \tag{2}$$

In this form, A is a constant, and the slope of $ln(I)$ - $E^{0.5}$ lines, $\alpha = \beta_s/kT$, increases linearly with $1/T$. The high frequency dielectric constant of Ta2O5 dielectric is likely in the range from 5 to 7 [21]. At these conditions and 85 ºC the theoretical value of the slope is from 5.5E-4 $(m/V)^{0.5}$ to 4.5E-4 $(m/V)^{0.5}$, which corresponds to the experimental data.

I-E characteristics for T598 capacitors had $\alpha \sim$ 5.8E-4 $(m/V)^{0.5}$ at room temperature, ~ 4.95E-4 $(m/V)^{0.5}$ at 85 ºC and ~4.7E-4 $(m/V)^{0.5}$ at 105 ºC (see Fig. 5), which is close to the data obtained for T520/T525 capacitors.

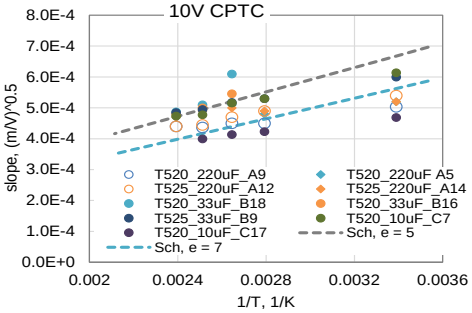

Fig. 4. Experimental (marks) and calculated per Schottky model (dashed lines) temperature dependencies of the slopes α.

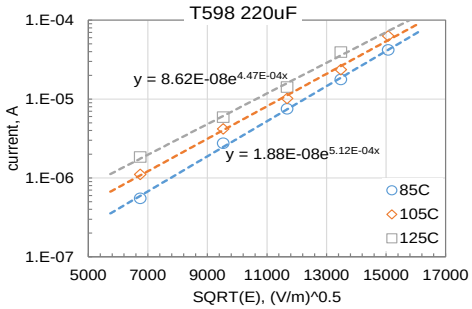

Fig. 5. *I-E* dependencies for median leakage currents of T598 220 µF capacitors at different temperatures.

Experimental data for the temperature dependence of the slopes of *I-E* characteristics are in a good agreement with calculations thus suggesting that the intrinsic leakage currents can be explained by the Schottky/Simmons model.

Effect of Temperature

Examples of temperature variations of leakage currents in T525 and T530 capacitors are shown in Fig. 6. In all cases experimental data in Arrhenius coordinates can be approximated with straight lines. The slopes of the lines that indicates activation energies of leakage currents, *U*, are decreasing with applied voltage, which is expected for the Schottky mechanism, Eq(1). For T520/T525 capacitors values of *U* at rated voltages varied from 0.1 eV to 0.18 eV. Similar activation energies, from 0.15 eV to 0.18 eV, were obtained for T530 150 µF and 220 µF capacitors. For T530 330 µF capacitors the value of *U* was somewhat higher, ~ 0.24 eV, which corresponds to the lower leakage currents for these parts.

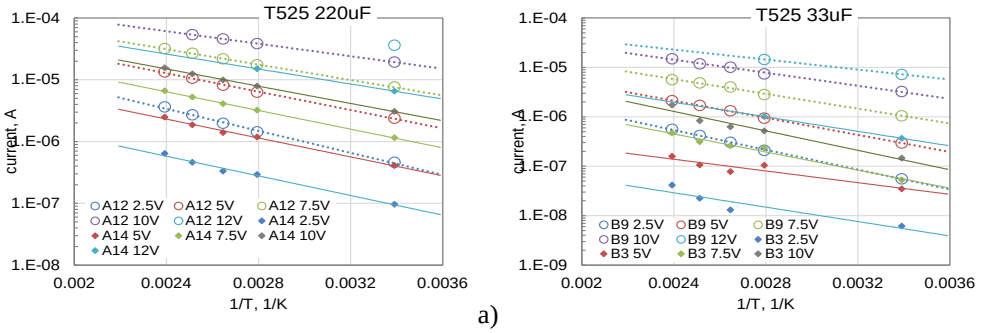

a) b)

Figure 6. Temperature dependencies of leakage currents for two samples at different voltages for T525 220 µF (a) and T525 33 µF (b) capacitors. Samples A12 and A14 (a) and B9 and B3 (b) represent capacitors with relatively low and high leakage currents.

Measurements using different types of CPTCs show that the activation energies decrease with applied voltage. To verify the applicability of the Schottky model, experimental and calculated data per Eq.(1) are displayed on Fig. 7a. Calculations have been made in an assumption that $\varepsilon = 5$ and $\Phi_B = 0.3$ eV (bottom line) and $\varepsilon = 7$ and $\Phi_B = 0.35$ eV (top line in Fig. 7a). Fig. 7b shows variations of U with electric field for two samples of T598 capacitors. A linear approximation of the data in U vs. $E^{0.5}$ coordinates shows that 0.35 eV < Φ_B < 0.4 eV and the slope is in the range from 1.25E-5 eV×(m/V)$^{0.5}$ to 1.36E-5 eV×(m/V)$^{0.5}$. Note that the theoretical value of the slope (β_s/q) is slightly larger, 1.7E-5 eV×(m/V)$^{0.5}$ at $\varepsilon = 5$ and 1.43E-5 eV×(m/V)$^{0.5}$ at $\varepsilon = 7$. However, considering uncertainties in the dielectric thickness and dielectric constant at high frequencies, this discrepancy is not significant.

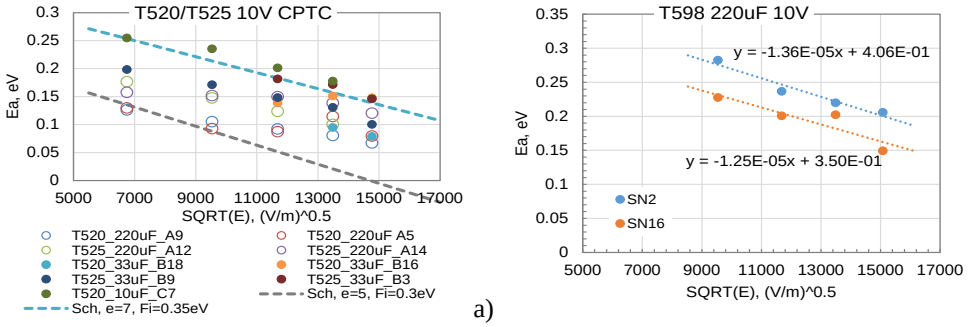

a) b)

Figure 7. Effect of electric field on activation energy of leakage currents for T520 and T525 capacitors (a) and T598 capacitors (b).

Table 2 summarizes experimental data for activation energies determined at the rated voltage and estimated values of the barrier heights for different types of CPTCs rated to 10 V. It should be noted that low activation energies are most likely specific for low-voltage polymer capacitors. For high voltage polymer hermetically sealed capacitors U was in the range from 0.75 eV to 0.88 eV [22].

Table 2. Activation energies for leakage currents in 10 V polymer tantalum capacitors.

Part Type	T520/T525	T530	T598
***U* at 10V, eV**	0.15 ±0.05	0.19 ±0.04	0.2 ±0.03
Φ_B, eV	0.3 – 0.35	0.3 – 0.35	0.35-0.4

DEGRADATION OF LEAKAGE CURRENTS DURING HALT

Monitoring of leakage currents during HALT showed that currents are gradually increasing with time. Typical variations of currents with time of testing for different part types are shown in Fig. 8. A portion of the *I-t* curve with increasing currents (typically after a few minutes of electrification) was approximated with a linear function:

$$I(t) = I_0 + \alpha \times t \tag{3}$$

where I_0 is the initial current, and α is the rate of degradation.

The voltage and temperature acceleration factors for reliability calculations were determined as a ratio of degradation rates at the test and operating conditions. The voltage acceleration factor, AF_V, can be written as an exponential function of voltage similar to what is used in MIL-PRF-55365 for the Weibull grading test, and temperature acceleration factor, AF_T, is based on Arrhenius law:

$$AF_V = \exp\left[B \times \left(\frac{V_{test}}{VR} - 1\right)\right], \qquad AF_T = \exp\left[\frac{E_a}{k} \times \left(\frac{1}{T_{op}} - \frac{1}{T_{test}}\right)\right], \tag{4}$$

where B is the voltage acceleration constant (assumed to be 18.8 for MnO2 capacitors per MIL-PRF-55365), k = 8.617×10−5 eV/K is the Boltzmann constant, and E_a is the activation energy of the degradation process.

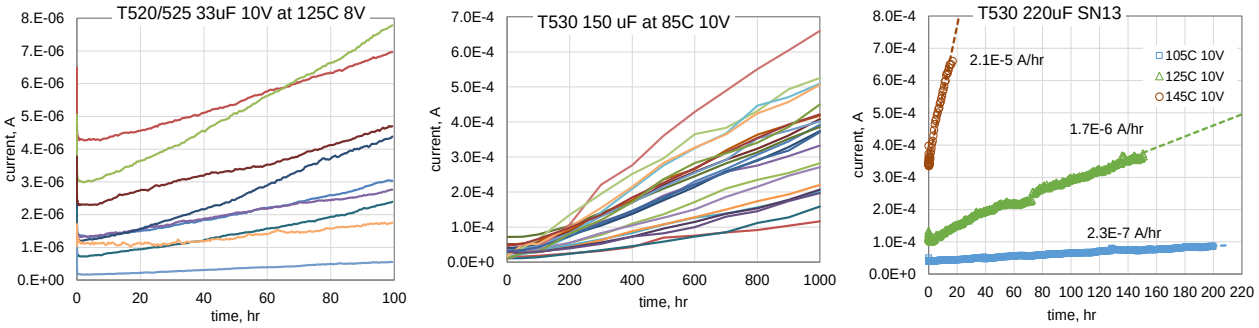

a) b) c)

Fig. 8. Examples of degradation of leakage currents with time during HALT. (a) T520/T530 33 µF capacitors at 125 ºC, 8 V; (b) T530 150 µF capacitors at 85 ºC, 10 V during 1000 hours life testing; (c) Degradation of leakage currents for one sample of the T530 220 µF capacitors tested consequently at 105 ºC, 125 ºC, and 145 ºC.

Technique

The method used for analysis of degradation in CPTCs was similar to the one used previously for MnO2 capacitors [23]. Rates of current degradation were calculated for each part at each test condition and distributions of α were approximated with Weibull functions.

Slopes of the distributions, β, and the scale parameters, η, were determined using a general log-linear model at a reciprocal transformation of absolute temperature. ALTA-7 software available from ReliaSoft was used to calculate parameters of the model based on the maximum likelihood estimation (MLE) method. According to this method, all distributions are assumed to have the same slopes, and the scale parameter depends on temperature and voltage as:

$$\eta(T,V) = a_0 \times \exp\left(\frac{a_1}{T}\right) \times \exp\left(a_2 \times V_{test}\right), \tag{5}$$

where a_i are parameters of the model, and T is the absolute temperature.

Based on the model's parameters, the voltage acceleration constant, B, and the activation energy of degradation, E_a, can be calculated: $B = a_2 \times VR$ and $E_a = -a_1/k$.

Monitored HALT had been carried out for different part types on groups of 10 to 22 samples at conditions shown in Table 3.

Table 3. HALT condition matrix.

T/V	85 ºC /10V	105 ºC /8V	105 ºC /10V	125 ºC /8V	125 ºC /10V	125 ºC /12V	145 ºC /10V	145 ºC /10V
T520 220uF			X	X	X			
T525 220uF			X	X	X		X	
T520 33uF		X	X	X	X		X	
T525 33uF			X	X	X		X	
T520 10uF			X	X	X	X	X	
T530 330uF	X				X		X	X
T530 220uF	X				X		X	X
T530 150uF	X		X		X		X	

T598 220uF					X	X	X	

HALT results

Examples of *I-t* characteristics during monitored HALT for different groups of capacitors are shown in in Fig. 9. In all cases currents are increasing with time under stress and in some cases raised more than two orders of magnitude during 100 hours of HALT. In most cases currents increased with time linearly; however, for some part types there was a trend of current saturation with time.

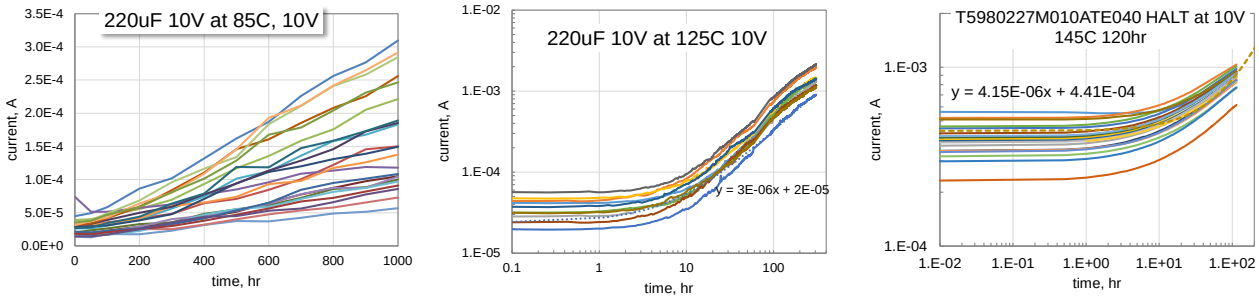

a) b) c)

Fig. 9. Degradation of leakage currents during HALT for different groups of CPTCs. (a) T530 220 µF capacitors at 85 ºC 10 V; (b) T530 220 µF capacitors at 125 ºC 10 V; (c) T598 capacitors at 145 ºC 10 V.

Distributions of the degradation rates at different test conditions are displayed in Weibull coordinates in Fig. 10. Marks on the plots correspond to the experimental values and lines represent distributions calculated according to the model per Eq.(5). Note that the general log-linear model was used for all groups except for T530, where testing at different temperatures were carried out at the rated voltage only. For these parts, the Arrhenius Weibull model was employed.

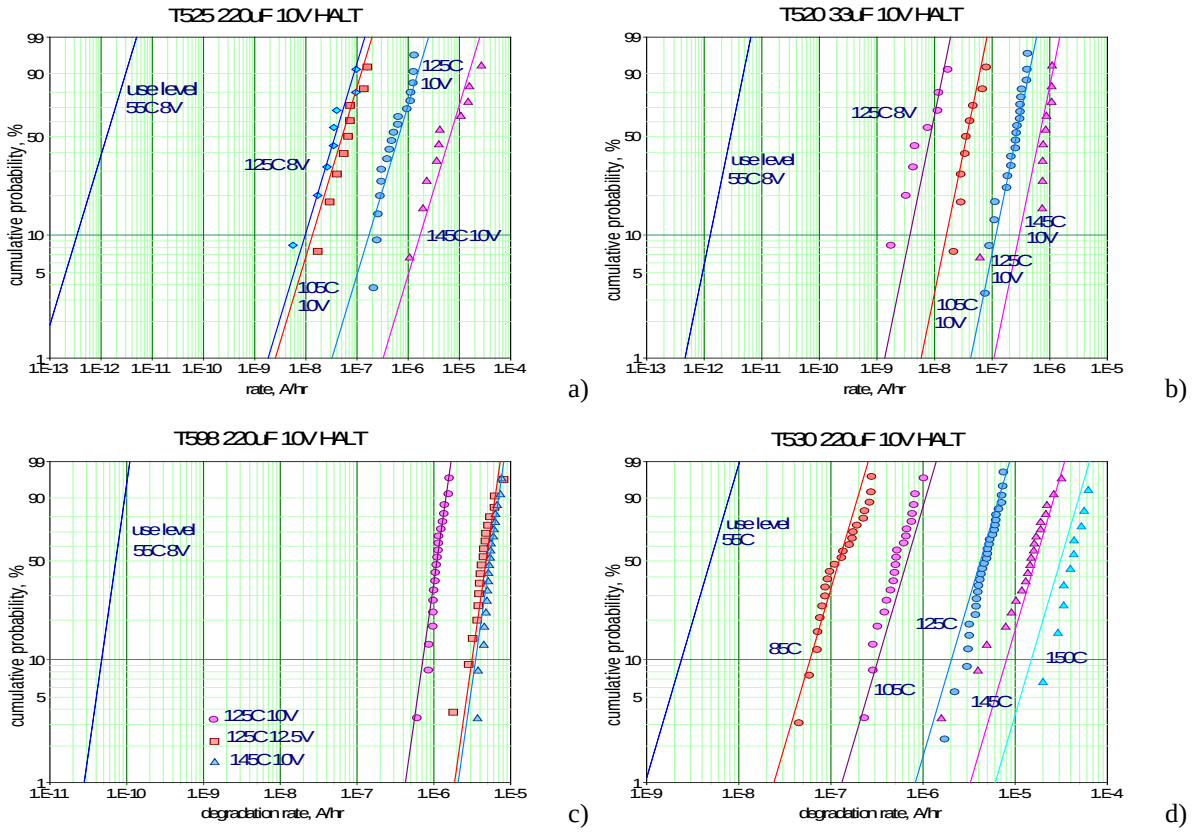

a) b) c) d)

Fig. 10. Experimental (marks) and calculated per the model Eq.(5) distributions of the degradation rates for different part types.

Results show that the model simulates experimental data accurately enough, so it can be used for prediction of degradation rates at operating conditions. The operating conditions for calculations below are assumed at T_{use} = 55 ºC, and V_{use} = 8 V (80% derating).

Assuming that parametric failures of the parts occur when DCL reaches 200% of the initial limit, the time to failure can be calculated as:

$$TTF = \frac{\Delta I_{cr}}{\alpha} \ . \tag{6}$$

where $\Delta I_{cr} = DCL_{max}$ is the critical level of the current increase.

For 220 µF capacitors having α = 5E-9 A/hr calculations yield *TTF* ~ 5 years, which might be not acceptable for long-term missions.

Voltage acceleration constants *B* and activation energies of the degradation rate for all tested groups are shown in Table 4. The value of *B* for different types of CPTCs varies from 12.9 to 17.8. The average value is 15 and standard deviation 2. An average activation energy of the degradation rate is 1.27 eV at a standard deviation of 0.19 eV.

Table 4 shows also the 99th percentile of α at 55 ºC and operating voltages of 10 V and 8 V, and the relevant times to failure for 1% of the parts. At 8 V and 55 ºC the calculated *TTF* for all part types is greater than 10 years, and for some part types might exceed thousands of years. However, due to high activation energy of the degradation process, even a relatively minor increase in temperature might result in early failures. For example, at 65 ºC failures in T530 150 µF capacitors would be observed in less than 3 years.

Table 4. Voltage acceleration parameter, activation energy, and calculated times to failure.

part type	C, µF	*B*	E_a, eV	99% rate at 55 ºC 10V, A/hr	99% rate at 55 ºC 8V, A/hr	TTF at 55 ºC 10V, year	TTF at 55 ºC 8V, year
T520	220	12.9	1.28	5.2E-09	3.9E-10	4.8	64.4
T525	220	14.3	1.65	8.7E-11	4.9E-12	289	5125
T520	33	17.2	1.28	2E-10	6.5E-12	18.8	579.6
T525	33	14.6	1.2	9.3E-10	5E-11	4.1	75.3
T520	10	17.8	1.27	5E-11	1.4E-12	22.8	815.4
T530	330	N/A	1.5	1.3E-10	6.5E-12*	290	5796*
T530	220	N/A	1.09	1.1E-08	5.5E-10*	2.3	45.7*
T530	150	N/A	1.06	3.3E-08	1.7E-09*	0.5	10.4*
T598	220	13	1.13	1.4E-09	1.1E-10	17.9	228.3

*Estimations in assumption *B* = 15.

Analysis of *I-t* characteristics during HALT revealed anomalous behavior in some capacitors that manifested as a relatively fast increase (within hours) followed by a sharp decrease in leakage currents. Examples of such behavior are shown in Fig. 11. The spiking seems to occur on the top of a gradual degradation of leakage currents that still allows for calculations of the average degradation rate as it is shown in Fig. 11a. Although some level of spiking can be observed in several samples in most of the tested lots, it happens more often for T520 33 µF capacitors, and was not observed for T598 220 µF capacitors.

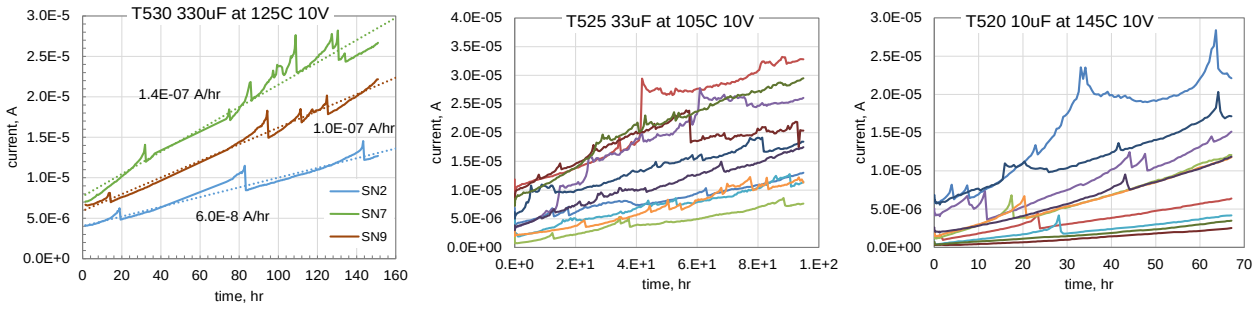

a) b) c)

Fig. 11. Anomalies (spiking) in current degradation during HALT.

Step Stress Testing at 85 ºC

To assess conditions that might cause catastrophic failures of polymer capacitors, T520 and T525 groups of parts that passed HALT at 125 ºC 12 V for 100 hours have been subjected to step stress testing. During this test, leakage currents at 85 ºC were monitored by voltage drop across 100 ohm resistors connected in series with each capacitor. The voltage was increased from 12 V to 20 V in 2 V increments, and duration of each step was 20 hours. Note that measurements of breakdown voltages for T520/T525 capacitors showed average VBR in the range from 19 V to 21 V for 220 µF and 33 µF capacitors and 24 V for 10 µF capacitors. The standard deviations for all groups varied from 1 V to 2 V.

Due to high leakage currents in 220 µF capacitors, seven T520 and one T525 capacitor were disconnected during 16 V step without catastrophic failures, so they were not tested at 18 V and 20 V. As a result, no catastrophic failures were observed with T520 capacitors that had the highest leakage currents. T525 220 µF capacitors were tested at 18 V for ~1 min and then the testing was stopped due to high leakage currents, but one part failed at 1.2 ohm.

Failures in 33 µF capacitors happened at 18 V only. However, a substantial increase in spiking was observed for these capacitors when voltage increased from 14 V to 16 V (see Fig. 13). At 18 V almost all parts failed short circuits within one hour of testing. One out of 20 samples of 10 µF capacitors failed after 13 hours at 18 V and 3 more failed within one hour of testing at 20 V. After that the testing was stopped. Similar to 33 µF capacitors, raising test voltages from 14 V to 18 V increased spiking in 10 µF parts substantially.

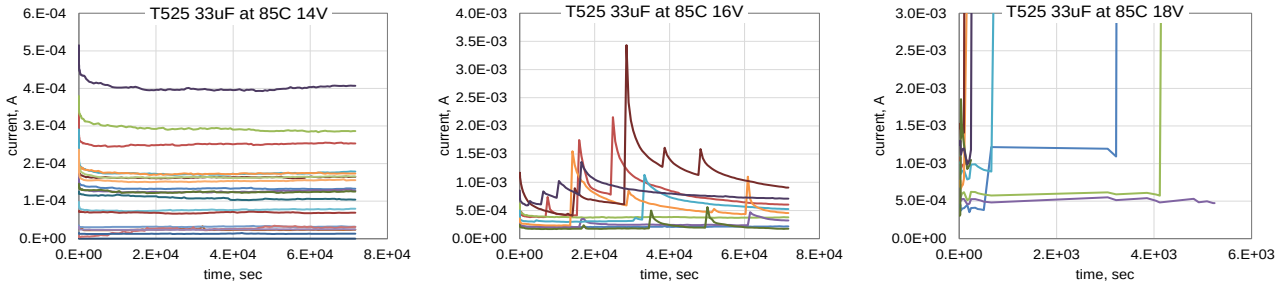

a) b) c)

Fig. 13. Variations of currents with time during 20 hour step stress testing at 85 ºC and increasing voltages for T525 33 µF capacitors at 14 V, 16 V, and 18 V.

EFFECT OF VACUUM ON CHARACTERISTICS OF TANTALUM CAPACITORS

To evaluate the effect of vacuum, three groups of T530 and one group of T525 220 µF capacitors were stored in a thermal vacuum chamber at a pressure of ~ 1E-7 torr and temperature 100 ºC for 1900 hours. Interim measurements of AC and DC characteristics were taken after 72 hr, 220 hr, and 540 hours of storage. For comparison, two groups of MnO2 capacitors, T510 330 µF 10 V multianode capacitors and CWR29 220 µF 10V military grade capacitors, were used. Results of vacuum testing showed no significant degradation of AC and DC characteristics in any of the groups. No changes in performance of MnO2 capacitors was observed during storage in both, vacuum and air chambers.

Considering that the rate of possible degradation at lower temperatures should be substantially lower, these results suggest that polymer tantalum capacitors might sustain long-term vacuum conditions and could be used in space applications.

To compare the effect of HTS at 100 ºC in vacuum and in air, two group of polymer (T530 150 µF and T525 220 µF) and two groups of MnO2 (T510 330 µF and CWR29 220 µF) capacitors have been stored for 1900 hours in a regular temperature chamber. Variations of AC characteristics (average values and standard deviations of the ratio of final and initial values) are shown in Table 5. No substantial degradation of C and DF in polymer capacitors was observed during storing in air. However, ESR values increased substantially, by 250% in T530 and by 35% in T525 capacitors, whereas no significant variations was observed after storage in vacuum conditions. Results indicate that space conditions might be beneficial for polymer tantalum capacitors.

Table 5. Results of HTS in vacuum and air at 100 ºC for polymer and MnO2 capacitors.

	Polymer				MnO2			
	T530 150uF		T525 220uF		T510 330uF		CWR29 220uF	
	vac	air	vac	air	vac	air	vac	air
C/C_i, %	95.0	93.4	96.2	93.4	98.2	98.3	93.6	97.8
STD	0.4	0.3	0.3	0.6	0.0	0.0	0.5	0.4
DF/DF_i, %	44.5	58.6	64.3	97.3	77.9	77.3	100.9	154.6
STD	2.5	1.4	1.5	16.6	2.0	1.1	6.8	12.5
ESR/ESR_i, %	116.8	359.0	90.3	134.3	96.9	83.6	96.1	89.2
STD	30.8	48.0	5.5	21.4	3.5	0.7	2.1	3.0

DEGRADATION OF AC AND DC CHARACTERISTIC DURING HTS

T530, T525 and MnO2 Capacitors During Long-Term HTS at 100 ºC

HTS at 100 ºC in air that was carried out in parallel with vacuum testing has been extended to 5000 hours. Measurements showed that capacitance between 1900 and 5000 hours remained stable for all part types. However, DF and ESR in CPTCs showed evidence of degradation already after 1900 hours and increased substantially by 5000 hours. Results of this extended testing are shown in Fig.14 and Fig.15, where data for vacuum testing are shown for comparison. Now, the differences in degradation of DF in air and vacuum became more obvious. In vacuum, after 72 hours DF remains stable, whereas in air DF increased on average two times by 5000 hours. One sample in the T525 group exceeded the specified limit of 10%, and more failures might be expected as testing continues. No DF degradation during 5000 hours was observed for MnO2 capacitors.

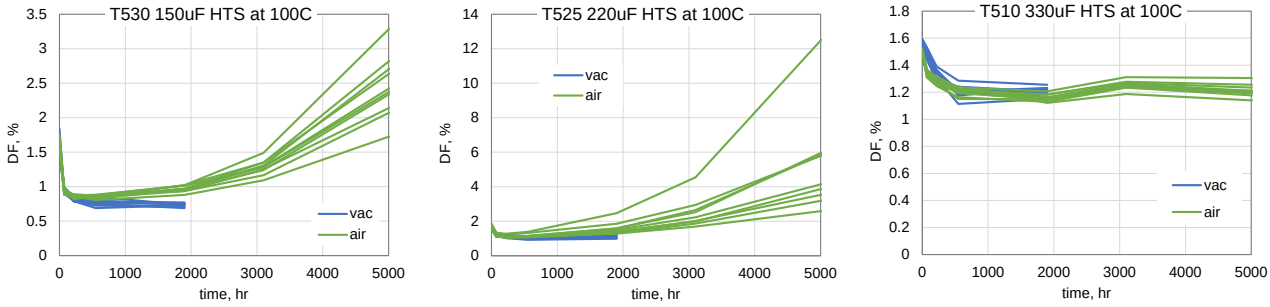

a) b) c)

Fig. 14. Variation of dissipation factor during storage at 100 ºC for polymer (a, b) and MnO2 (c) capacitors.

The difference in variations of ESR for MnO2 and polymer capacitors is also significant. T530 capacitors increased ESR by 5000 hours more than an order of magnitude, and T525 capacitors more than two times, whereas no substantial variations of ESR occurred for MnO2 capacitors.

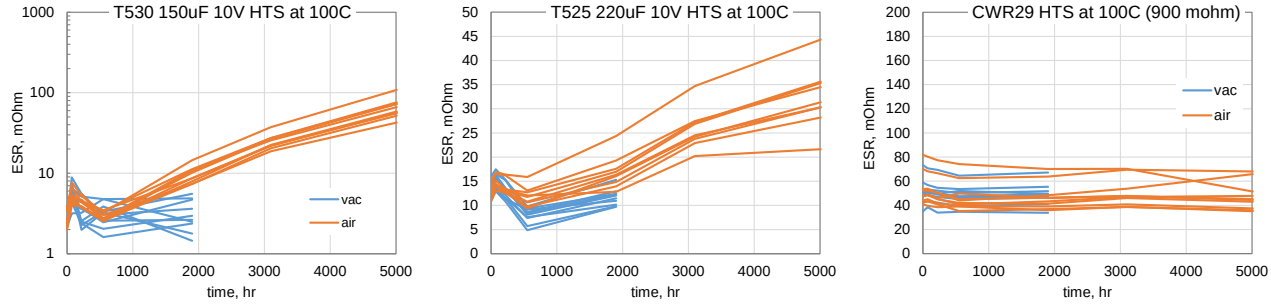

a) b) c)

Fig. 15. Variation of ESR during storage at 100 ºC for polymer (a, b) and MnO2 (c, d) capacitors.

Values of leakage currents measured after 1000 sec of electrification are plotted against the time of storage in Fig. 16. In both groups of CPTCs leakage currents decreased gradually at a rate ranging from 2E-10 A/hr to 3E-9 A/hr. No changes of DCL was observed in MnO2 capacitors.

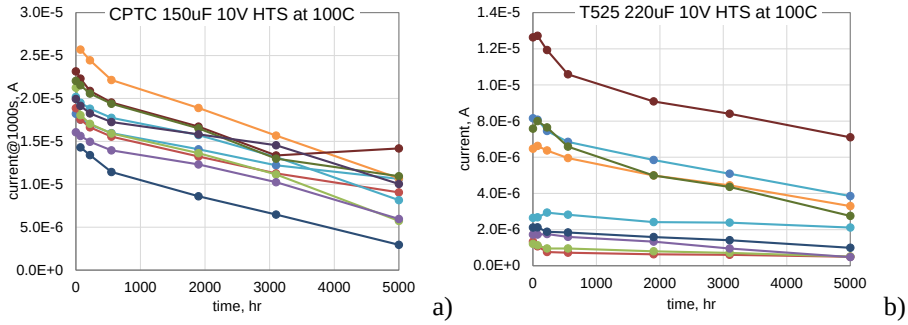

a) b)

Fig. 16. Variations of leakage currents with time at HTS 100 ºC for T530 150 µF (a) and T525 220 µF (b) capacitors.

Relaxation of currents measured at RT through the HTS testing at 100 ºC is shown in Fig.17. Initially, up to 1900 hours no anomalies were observed and currents remained stable during 40 min of testing under bias (Fig. 17a). However, measurements after 3100 hours showed that in one out of ten tested parts the current increased sharply after ~ 1500 sec, and then decreased with time (Fig. 17b). After 5000 hours of storage most of the parts had erratic behavior of leakage currents (Fig. 17c). No such spiking was observed for T525 capacitors. Note that leakage currents did not exceed the specified limits, and formally no failures occurred. However, if such a part is used for filtering purposes, burst-like noise and instability of leakage currents that results in sharp variations of currents might create excessive noise in the system instead of smoothing the signal and reducing possible ripple voltages.

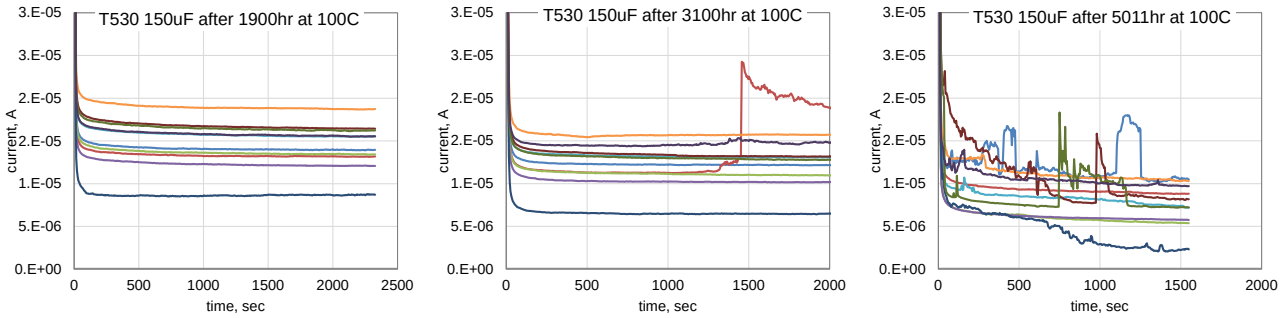

a) b) c)

Fig. 17. Relaxation of leakage currents after application of rated voltages (10 V) for T530 150 µF capacitors after 1900 (a), 3100 (b), and 5000 (c) hours at 100 ºC.

T530, T525 and MnO2 Capacitors During HTS at 125 ºC, 150 ºC, and 175 ºC

Different groups of T530 and T525 capacitors were stressed by HTS at 125 ºC for 1000 hours and then at 150 ºC for 1000 hours more. HTS testing at 175 ºC was carried for 310 hours.

Results of testing at 125 ºC (see Fig. 18) showed no significant degradation for MnO2 capacitors. Capacitance in CPTCs also remained relatively stable. However, five out of 10 samples of T525 220 µF and all T530 capacitors increased DF substantially after 500 hours of storage. One out of five T525 samples reached the limit of 10% by 1000 hours and 4 samples exhibited increased DF by 3 to 8 times. It is important to note that 5 out of 10 samples remained stable and showed no signs of degradation.

All T530 150 µF capacitors, except for one that remained stable, exhibited increased ESR significantly above the limit of 6 mohm after 500 hours of storage. However, no substantial variations of ESR was observed in T525 220 µF capacitors. This means that the mechanism of degradation for DF and ESR might be different. Results indicate also that the probability of degradation in CPTCs is lot-related.

Similar to HTS at 100 ºC, ageing at 125 ºC resulted in some decrease of leakage currents (measured at 1000 sec) with time of storage. However, no spiking or anomalies in current relaxation was observed. It is possible that a longer exposure to 125 ºC is necessary to initiate erratic behavior of leakage currents. As it will be shown below, spiking was observed in these parts after HTS at 150 ºC.

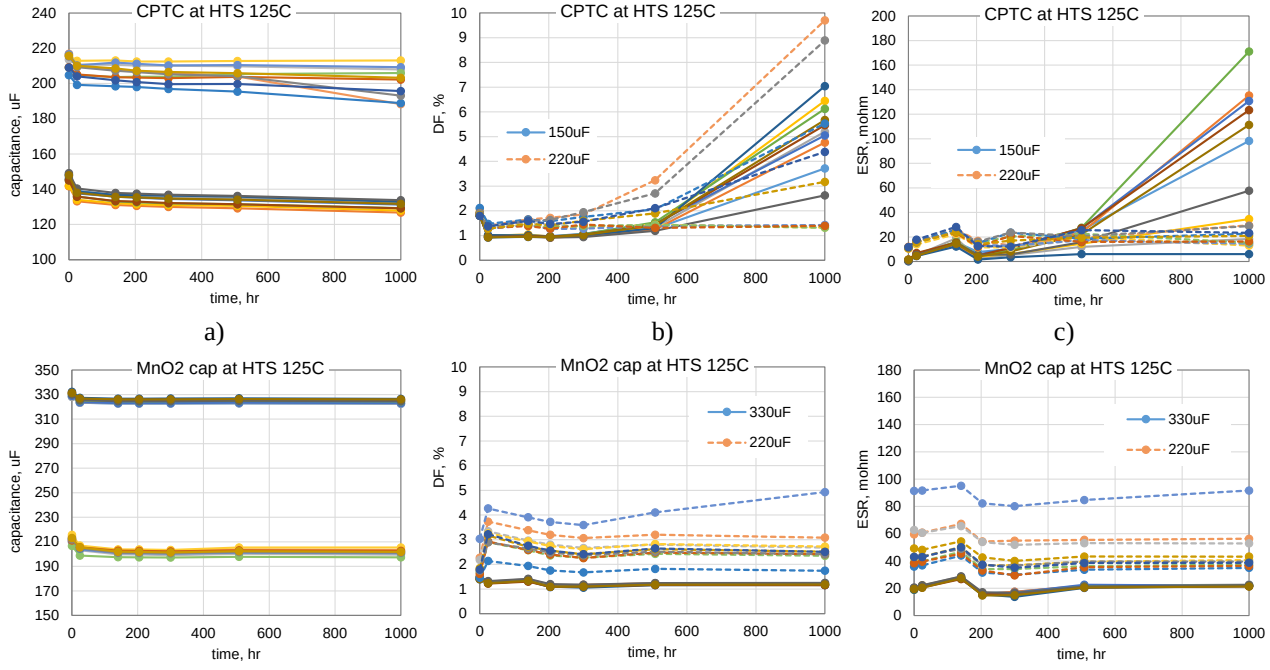

Fig. 18. Variation of AC characteristics during high temperature storage at 125 ºC for polymer (a-c) and MnO2 (d-f) capacitors (solid lines: T530 150 µF, dashed lines: T525 220 µF capacitors).

Measurements of frequency dependencies of capacitance and ESR for parts after HTS 125 ºC showed that although no significant decrease in capacitance was measured at 120 Hz for CPTCs, the roll-off frequency decreased substantially, which can be explained by the reduction of conductivity of the polymer. This can also explain increasing ESR that was more significant for T530 than for T525 capacitors. All T530 capacitors increased ESR more than 20 times, whereas only five out of ten T525 capacitors increased ESR from 2 to 3 times.

Storage at 150 ºC resulted in a substantial decrease of capacitance after 300 hours in five out of ten samplers of T525 and in all samples of T530 capacitors (see Fig. 19). Same samples of T525 capacitors that remained stable during storage at 125 ºC had stable capacitance during HTS at 150 ºC. Four out of these five samples had stable DF and ESR values. Degradation of DF in T530 capacitors, started after ~100 hours and of ESR after ~200 hours. By 1000 hours both parameters increased from 10 to 1000 times. All AC characteristics remained stable for both types of MnO2 capacitors during 1000 hours of storage at 150 ºC.

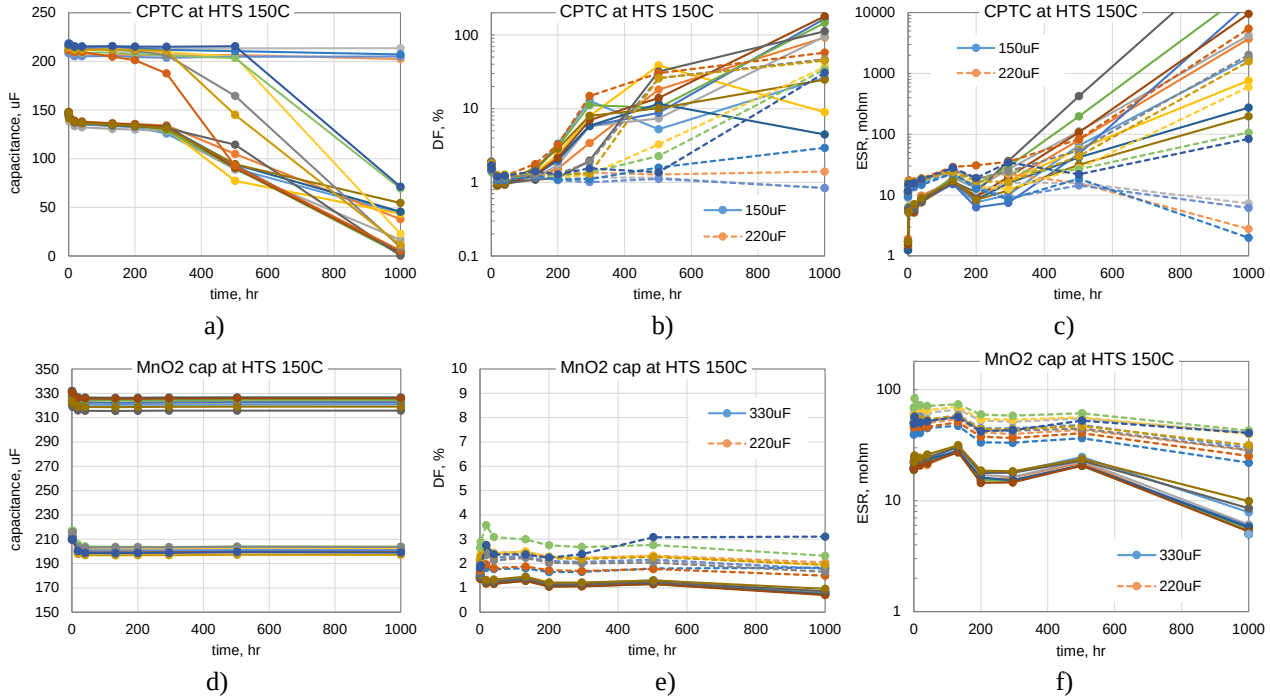

Fig. 19. Variation of AC characteristics during high temperature storage at 150 ºC for polymer (a-c) and MnO2 (d-f) capacitors (solid lines: T530 150 µF, dashed lines: T525 220 µF capacitors).

Changes in frequency dependencies of C and ESR after HTS at 150 ºC were similar to post-HTS 125 ºC measurements, but the level of degradation was much more severe. Four T525 samples had values of capacitance close to those measured initially, but evidences of degradation – decreasing of roll-off frequency and increasing ESR values were observed in all samples.

HTS at 150 ºC resulted in more significant changes of leakage currents compared to HTS 125 ºC. Fig. 20a shows correlation between initial and post-HTS 150 ºC currents measured after 1000 sec of electrification. Polymer capacitors exhibited reduced currents by one to two orders of magnitude, whereas no substantial changes were observed for MnO2 capacitors. Before HTS, leakage currents in polymer capacitors were stabilizing after a few dozens of seconds, but after HTS currents continue decreasing indicating the prevalence of absorption currents over the intrinsic leakage currents (see Fig. 20b and 20c). HTS resulted also in a substantial increase in instability and spiking of leakage currents.

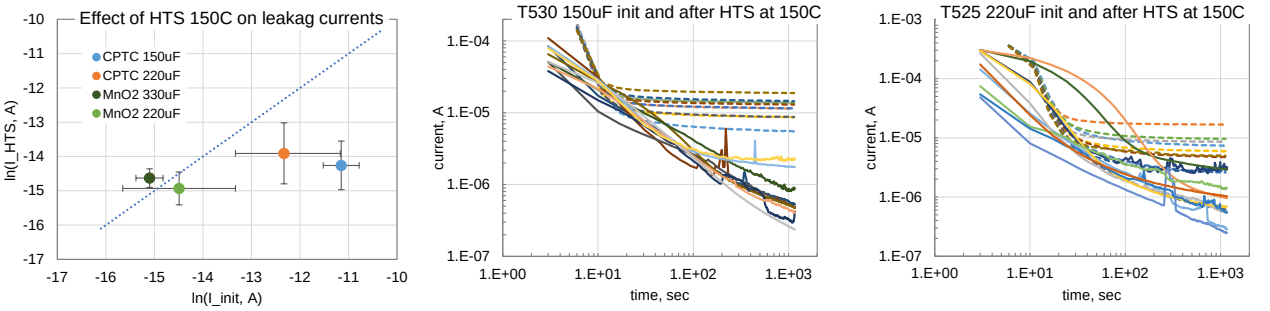

Fig. 20. Effect of HTS at 150 ºC for 1000 hours on leakage currents. (a) Correlation between initial and post-HTS leakage currents (marks indicate median values and error bars standard deviations). (b and c) Relaxation of leakage currents for T530 150 µF (b) and T525 220 µF (c) capacitors (dashed lines correspond to the initial measurements).

Automotive Grade Capacitors During HTS at 125 ºC and 150 ºC

Automotive grade, part type T598, 220 µF capacitors were stored at 125 ºC for 2000 hours and then for 1000 hours at 150 ºC. Note that that the specification for this part and AEC-Q200 require only 1000 hour testing at 125 ºC.

Results of this testing showed that all AC characteristics remained stable at both, 125 ºC and 150 ºC storage conditions. In spite of some spread of ESR values during HTS at 150 ºC, all parts remained within the specified limits (40 mohm).

Contrary to AC characteristics, leakage currents measured after 1000sec of electrification increased substantially. After HTS at 125 ºC leakage currents raised more than ten times and up to two orders of magnitude after HTS at 150 ºC (see Fig. 21a). One month storage at room conditions after HTS 125 ºC practically restored initial values of leakage currents.

Measurements of current relaxations showed that before HTS leakage currents were stabilizing after ~ 100 sec of polarization; however, no stabilization was observed after HTS for at least 1200 sec and currents continue decreasing gradually with time under bias (see Fig. 21b). This might suggest increasing absorption currents; however, the level of depolarization currents did not change and was 2 to 3 orders of magnitude below the polarization currents. Also, the slope of *I-t* characteristics under bias was relatively small and values of *n* decreased from ~0.45 after HTS at 125 ºC to ~0.3 after HTS at 150 ºC, whereas depolarization currents remained unchanged with the slope close to 1 even after 2000 hours of HTS at 125 ºC (see Fig. 21c).

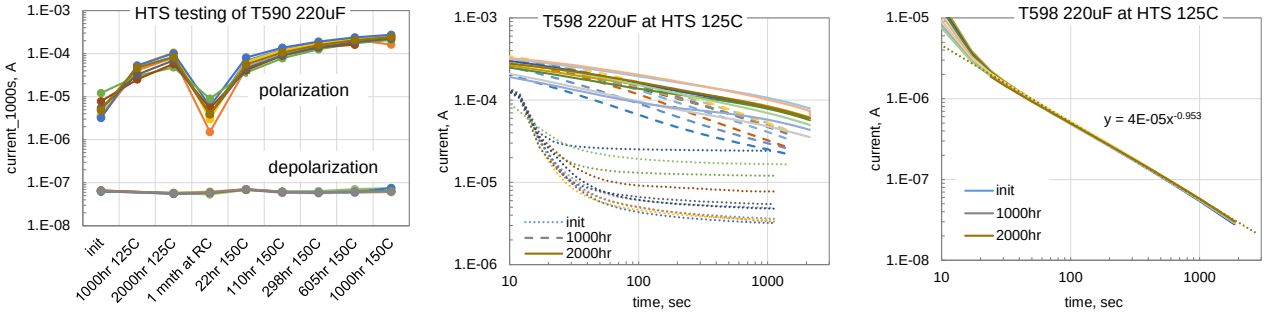

a) b) c)

Fig. 21. Effect of HTS on leakage currents in T598 capacitors. (a) Variations of currents measured after 1000 sec through the testing. (b, c) Relaxation of leakage currents during polarization at 10 V (b) and depolarization at 0 V (c).

Degradation Model for HTS

Based on the degradation kinetics of AC characteristics, times to parametric failures were calculated at different temperatures for T530 150 µF and T525 220 µF capacitors. Because of a large margin between the actual values of DF (1% to 2%) and the limits (typically 10%), *TTF* was estimated at times when DF increased three times compared to the initial values. ESR failures were determined at conditions ESR = 3×ESR_{limit}. Results of calculations are shown in Fig. 22 where *TTF* values for each temperature were approximated with Weibull distributions. Because we are mostly interested in early failures, the approximating functions were selected to describe a subgroup of capacitors with small TTF values.

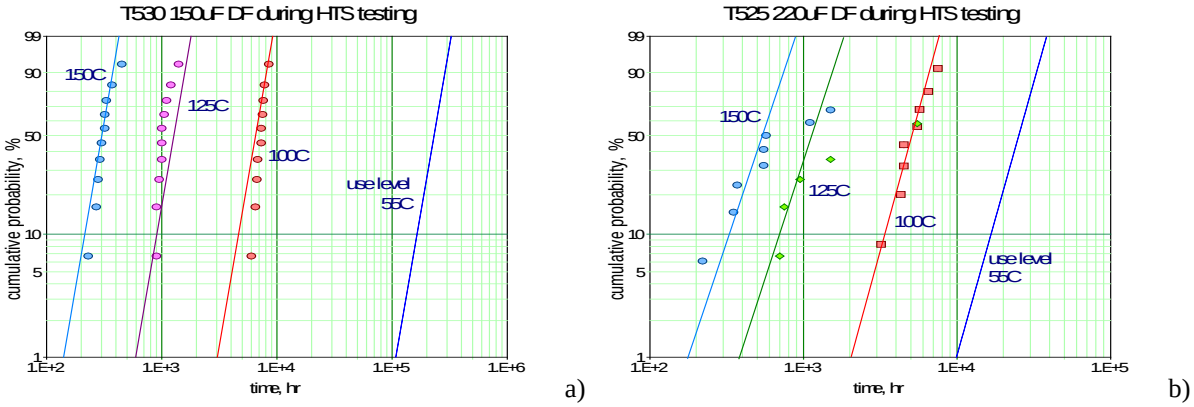

a) b)

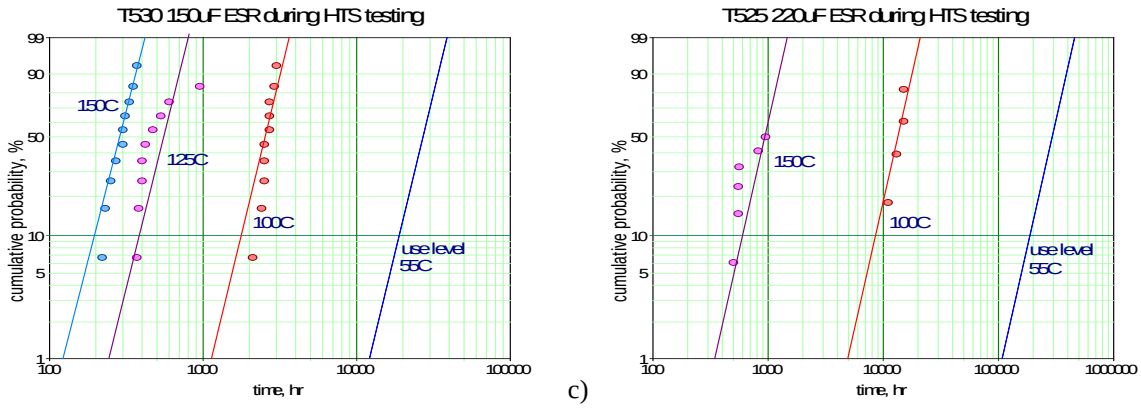

Fig. 22. Distributions of times to parametric failures for T530 150 µF (a, c) and T525 220 µF (b, d) capacitors.

Median *TTF* values are plotted against temperature in Arrhenius coordinates in Fig. 23 to estimate effective activation energies of the degradation processes. Estimations show that activation energies are in the range from 0.5 eV to 0.85 eV.

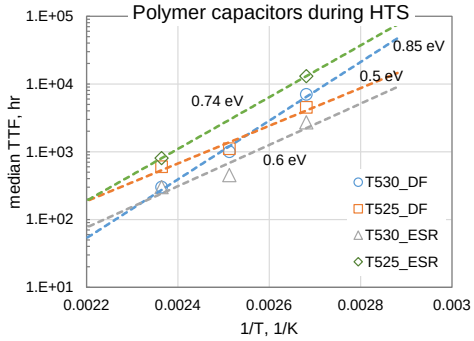

Fig. 23. Variation of median time to parametric DF and ESR failures with temperature.

Using Arrhenius' law, predictions of times to failure at 85 ºC and maximum temperatures that would allow storing the parts for 10 years without parametric failures have been calculated (see Table 6). Storage of T530 and T525 capacitors even at a relatively low temperature of 85 º C might result in parametric failures within a few years. For 10 year operation of these parts, the environmental temperature should not exceed ~ 40 ºC.

Although no parametric failures was observed for T598 capacitors, we can estimate *TTF* by assuming that the mechanism of degradation is similar for all 10 V capacitors. Assuming E_a = 0.7 eV and based on the fact that no parametric failures happened during 2000 hours at 125 ºC and 1000 hours at 150 ºC, calculations show that automotive grade T598 capacitors can operate at 85 ºC in air for more than 6 years. Considering that the rate of degradation in vacuum is substantially less than in air, these part most likely can operate in space for more than 10 years.

Table 6. Activation energies for parametric degradation of CPTCs during HTS in air and estimations for *TTF* at 85 ºC and maximum temperature during 10 year storage.

	T530_DF	T525_DF	T530_ESR	T525_ESR	T598_ESR
E_a, eV	0.85	0.5	0.6	0.74	0.7*
TTF_{median} at 85 ºC, year	2.21	0.88	0.57	3.92	>6*
T_{max} for 10 year operation	70 ºC	38 ºC	43 ºC	71 ºC	

*expected values

DISCUSSION AND RECOMMENDATIONS

Failures due to AC or DC parameters being out of the specification caused by environmental stresses might happen in both MnO2 and polymer tantalum capacitors. However, MnO2 chips have much better stability during HTS compared to CPTCs. The existing quality assurance (QA) system for MnO2 capacitors is focused mostly on elimination of catastrophic, short circuit failures. These failures rarely happen with polymer capacitors, and these parts require a different approach for QA.

Degradation of Leakage Currents During HALT

The mechanism of degradation of leakage currents in polymer capacitors under bias is likely similar to what was observed in MnO2 capacitors and is related to migration of oxygen vacancies, V_o^{++}, in Ta2O5 dielectrics [23]. The activation energy of the degradation rate can be presented as a sum of activation energy of leakage currents, U, and activation energy of the migration process, E_v:

$$E_a = U + E_v \,, \tag{7}$$

The values of U are in the range from 0.1 eV to 0.23 eV, and E_a varies from 1.1 eV to 1.3 eV. This yields E_v in the range from 0.9 eV to 1.2 eV, which is close to activation energies reported previously for MnO2 capacitors (~1.1 eV).

For polymer tantalum capacitors KEMET studies showed that activation energies for catastrophic wear-out failures at voltages ranging from the rated to 2.2VR decreased with applied voltage and were in the range from 1.8 eV to 0.87 eV [24-26]. At relatively low applied voltages, close to the rated, activation energies for catastrophic failures are much greater than for parametric failures analyzed in this study. Most likely, these two types of failures are due to different physical mechanisms. Catastrophic failures that might occur even without degradation of leakage currents are due to the time dependent dielectric breakdown (TDDB) [27], whereas parametric failures are caused by migration of oxygen vacancies. Note, that the TDDB model also predicts decreasing activation energy with applied voltage that can vary from 2.5 eV to 1 eV [27]. According to the thermochemical model of TDDB developed by McPherson [28], electrical breakdown in oxides occurs when the local electrical field weakens polar molecular bonds to the level at which thermal energy is sufficient to cause the breakage. This mechanism might be also related to the field-induced crystal growth in tantalum capacitors that is often used to explain failures in the parts. Weakening of the bonds might enhance crystal growth that eventually results in the rupture of the oxide.

It is important to note that similar to MnO2 capacitors, the rate of degradation in polymer capacitors has a trend of decreasing with time of testing. This might be explained by a limited amount of V_o^{++} in the dielectric or some compensation processes that neutralize accumulated positive charge with time (e.g. electron trapping). For this reason, predictions of the times to parametric failures based on the model are rather conservative.

Step stress testing experiments have shown that catastrophic failures during HALT can be observed with time at voltages close to breakdown. This indicates that similar to MnO2 capacitors, failures in polymer capacitors can be attributed to the TDDB mechanism [27]. Increasing test voltages result in a substantial increase of the probability of current spiking, and as voltages increase further, catastrophic failures occur. This indicates that spiking and the current noise are likely manifestations of local scintillation breakdowns creating damage to the dielectric that is not fully self-healed. The probability of spiking depends on the quality of dielectric and increases with time under bias indicating weakening of the dielectric strength during the testing.

Burn-In and Life test conditions

The purpose of burning-in is to remove infant mortality (IM) failures from the lot. For MnO2 capacitors that historically had a large proportion of IM failures, the Weibull Grading Test (WGT) is used. This test is the major quality assurance procedure for hi-reliability MnO2 capacitors that combines burning-in and failure rate qualification testing. Failures during WGT are due to short circuits in the parts and are detected as blown 1 A fuses connected in series with each capacitor.

CPTCs are more likely to fail parametrically due to increased leakage currents, and the probability of catastrophic IM failures for CPTCs is much less than for MnO2 capacitors, which is in agreement with KEMET data [13]. For this reason, WGT is not an effective test for polymer capacitors and should be replaced with a test that is specific to the behavior of CPTCs. One of such specifics is that parts might have unstable, erratically changing or spiking leakage currents. To address this specific issue, leakage currents in polymer capacitors during burning-in and life testing should be monitored and parts with excessive current spiking should be considered as failures. Also, the level of current degradation during BI or life testing should be limited. For space applications, monitored burning-in at 105 ºC, 1.1VR for 40 hours and monitored life testing at 105 ºC and rated voltages for 2000 hours can be recommended.

Effect of vacuum

Results show that moisture desorption in vacuum does not cause degradation in low-voltage polymer capacitors. More than that, stability of AC characteristics in vacuum is better compared to air environments. This is obviously due to thermal oxidation of polymers that is the major cause of PEDOT degradation. The significance of oxygen presence was also confirmed by studies of ageing and treatment of PEDOT and PEDOT/PSS polymers in air and nitrogen environments [29-31].

For space operations, estimations of TTF made based on HTS testing in air are rather conservative. In general, in environments without oxygen most polymer materials degrade with time significantly less that in air [32]. Based on results of studies of the thermal degradation of polystyrene (PS), polyethylene (PE), and polypropylene) (PP) in both inert nitrogen

and air atmospheres reported in [33], average activation energy of degradation reduced from ~2.3 eV in N2 to 0.7 eV in air for PE, from ~2.0 eV in N2 to 0.87 eV in air for PP, and from ~2.1 eV in N2 to 1.1 eV in air for PS. Note that activation energies of the thermo-oxidative degradation for these materials in air, from 0.7 eV to 1.1 eV, are close to the values obtained in this study.

One of the potentially negative effects of vacuum might be a reduction of the self-healing efficiency. If the self-healing process is due to the thermal oxidation of conductive polymers caused by local heating at the defect site, it might not occur in vacuum. In this case, spiking observed during HALT that is a manifestation of the self-healing process might be much more significant in vacuum or even result in catastrophic failures. This requires a thorough control of stability of leakage currents during BI and life testing for CPTCs intended for use in space.

Degradation of leakage currents during HTS

Storage in the temperature range from 100 ºC to 175 ºC showed no significant variations of currents in MnO2 capacitors. For polymer capacitors, changes of leakage currents with time of storage fall into three categories: (1) decreasing; (2) increasing; (3) currents became unstable (increase of spiking). All general purpose capacitors (T530 and T525) belong to the first category, whereas automotive grade, T598, capacitors belong to the second category. Spiking appears with time of storage in some parts that belong to the first category. One of possible reasons for increasing current instability is that high initial intrinsic currents in the parts mask the spiking, but it became obvious when leakage currents decrease.

Decreasing of leakage currents as a result of HTS is likely due to annealing processes that reduce concentration of defects, and in particular oxygen vacancies, in the tantalum pentoxide dielectric. A substantial reduction of leakage currents during annealing of Ta2O5 films in nitrogen [34] or oxygen [35] environments was attributed to removal of certain structural imperfections present in the dielectric initially.

Increasing leakage currents during HTS in T598 capacitors might be related to the difference in polymer materials used. It is possible that these parts were manufactured using a larger portion of PEDOT/PSS in the hybrid cathode system, whereas general purpose capacitors employ mostly in-situ polymerization.

Anomalous transient currents in capacitors with PEDOT/PSS cathodes have been observed before and explained in [9] by reorientation of dipoles in PEDOT and PSS macromolecules after voltage application. It is assumed that in the absence of moisture this reorientation occurs slowly, so it requires more time for current relaxation. Reorientation of dipoles changes the barrier at the polymer/Ta2O5 interface and thus affects leakage currents. Moisture plays a role of a plasticizer and accelerate orientation of dipoles substantially. This effect was not observed on high-voltage capacitors with pre-polymerized PEDOT/PSS electrodes and on capacitors with in-situ polymerization of PEDOT and is considered to be specific for hybrid capacitors only. The observed [9] transients occurred within less than a second, whereas we observed much longer, hours-range, relaxations. These slow processes are typically related to ionic, rather than to dipole relaxation in dielectrics.

The phenomenon of anomalously slow relaxation of leakage currents in dry capacitors with PEDOT/PSS cathodes was also observed in [8]. Similar to [9], relaxation was accelerated substantially in the presence of moisture. The effect was explained by formation of a dielectric layer on the surface of the cathode at the boundary with the dielectric. Part of the sulphonic groups in PSS, SO3H, is dissociated forming a negative charge, $SO3^-$, and a positive charge compensating PEDOT. After voltage is applied this negative charge moves towards the dielectric surface thus increasing the barrier and reducing leakage currents. In the presence of moisture the dissociation is enhanced and relaxation of currents occurs faster.

The existing models still do not explain all specifics of the anomalous transients, in particular, a substantial increase in current amplitudes, and require further analysis. Attributing the effect to moisture desorption only is not consistent with the diffusion kinetic in tantalum capacitors. The characteristic time of moisture diffusion at 125 ºC is 10 to 20 hours [36], whereas current continued increasing after 1000 hours of storage. It is possible that electron trapping processes in the dielectric play an important role in the current transient. Releasing of electrons from deep traps in the dielectric during HTS reduces the effective negative charge at the polymer/Ta2O5 interface resulting in decreasing of the barrier height and enhancing electron flow through the dielectric. Application of bias after HTS results in high initial currents that decrease slowly with time due to build up of negative charges of trapped electrons.

Degradation of AC characteristics during HTS

Degradation of AC characteristics is mostly due to decreasing of conductivity of PEDOT or PEDOT/PSS cathode systems as a result of thermo-oxidative processes in polymers. Cross-sectioning of samples after HTS (see Fig. 24) shows that the major path for oxygen penetration to the conductive polymer is along the lead-frame and anode riser wire. Thin discolored lines along the case surface and interfaces of molding compound with elements of capacitors indicate areas where the epoxy resin was decomposed by oxygen. Cracks in the case clearly provide a direct path for oxygen penetration that might accelerate degradation processes substantially, and contrary to MnO2 capacitors, pose a serious reliability risk. For this reason, improvements in quality of packaging was one of the major means for KEMET to assure stability of automotive

grade capacitors under environmental stresses [5]. Contrary to general purpose, T520, T525 and T530 capacitors, automotive grade capacitors had no degradation of AC characteristics during 2000 hr HTS at 125 ºC. This might be partially due to a more thorough control over the encapsulation process.

Cross-sectioning of the parts after HTS at 175 ºC (see Fig. 24 c, d) also reveal discoloration of molding compound along the surface of the case, at the entrance of the lead frames and anode riser wires. However, no evidences of decomposition along the tantalum slug and cathode contact pads were observed. Fig. 24c shows T525 220 µF SN23 capacitor that did not fail after the testing and the part in fig. 24d is T530 150 µF SN30 capacitor that failed marginally DF at 18% and ESR at 97 mohm. Note that the part shown in fig. 24a, T530 150 µF SN16, failed catastrophically at DF = 146% and ESR 23 ohm. A much less severe degradation after HTS at 175 ºC corresponds to the absence of discoloration in molding compound at the internal areas around the slug. Most likely, this is due to a much shorter duration of the stress at 175 ºC (300 hr) compared to 1000 hr at 150 ºC.

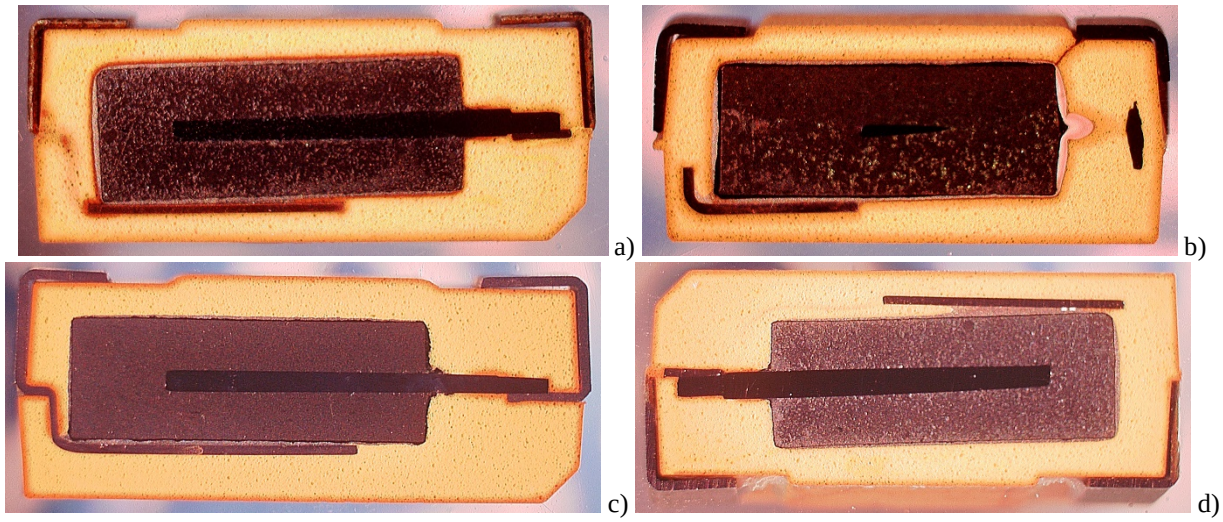

Fig. 24. Cross-sectional views for two CPTCs after HTS at 150 ºC for 1000 hr (a, b) and at 175 ºC for 300 hr (c, d). Note a thin layer of discoloration along the surface of the case and anode riser wires (all pictures), along the lead frame, (a) and (b) - the whole surface, and (c) and (d) – part of the area.

Kinetics of degradation of AC characteristics shows that there is an induction period before degradation starts. This period might be associated with the time necessary to cause delamination and allow a free path for oxygen penetration. It is also possible that a certain amount of oxygen should be accumulated at the interface to initiate thermo-oxidative processes and increase resistivity of PEDOT polymers. This might explain a better stability of hermetically sealed compared to chip capacitors. A limited amount of oxygen inside the can is likely not sufficient to cause degradation in conductive polymers.

Mechanisms of degradation of capacitance, ESR, and DF are different. Decrease in capacitance is related to increasing ESR and is due to reduction of the roll-off frequency. Increase in ESR can be attributed to three factors: (i) increasing resistance of the polymer, (ii) cracking in the polymer caused by the thermal decomposition and reduction of the polymer volume, and (iii) delamination between the cathode layers. Analysis shows that degradation of DF might be due to two factors: (i) increasing ESR and (ii) increasing of absorption processes due to generation of electron traps at the polymer/Ta2O5 interface. Examples of cracking and delamination in polymer capacitors after HTS at 150 ºC are shown in Fig. 25 and 26.

Maximum operating temperature for both high quality polymer and MnO2 capacitors is the same, 125 ºC. However, contrary to MnO2 capacitors that are stable even during long-term exposure to 150 ºC, characteristics of CPTCs might degrade substantially even at relatively benign environments, e.g. during long-term unbiased testing at 100 ºC. For this reason, HTS testing that is currently not required per MIL-PRF-55365, should be a part of QA for polymer tantalum capacitors. Testing at 125 ºC for 1000 hours (similar to AEC-Q200) can be recommended as a lot acceptance test and 10,000 hours testing at 100 ºC as a qualification test.

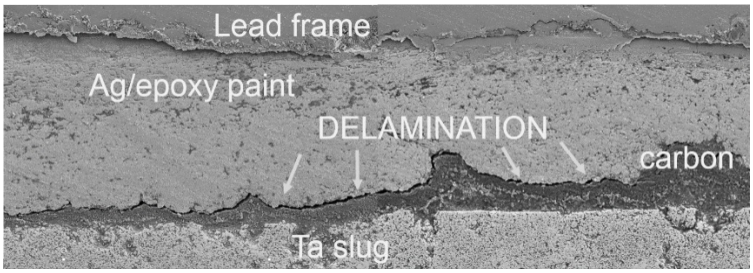

a)

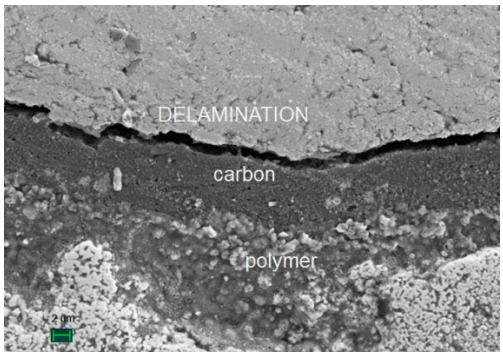

b)

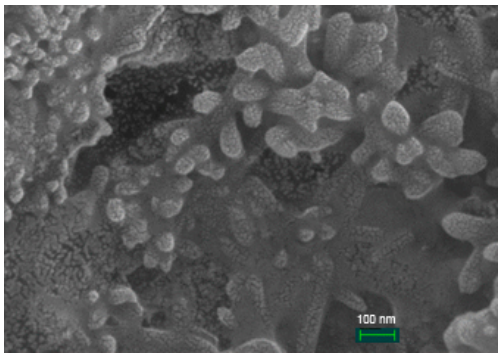

c)

Figure 25. SEM views of cross-sections of T530 330 µF SN34 capacitors after HTS at 150 ºC that fail ESR at 80 ohm showing delamination between the silver epoxy and carbon layers (a, b). Figure (c) shows close-up structure of the conductive polymer with nanometer size crystallites.

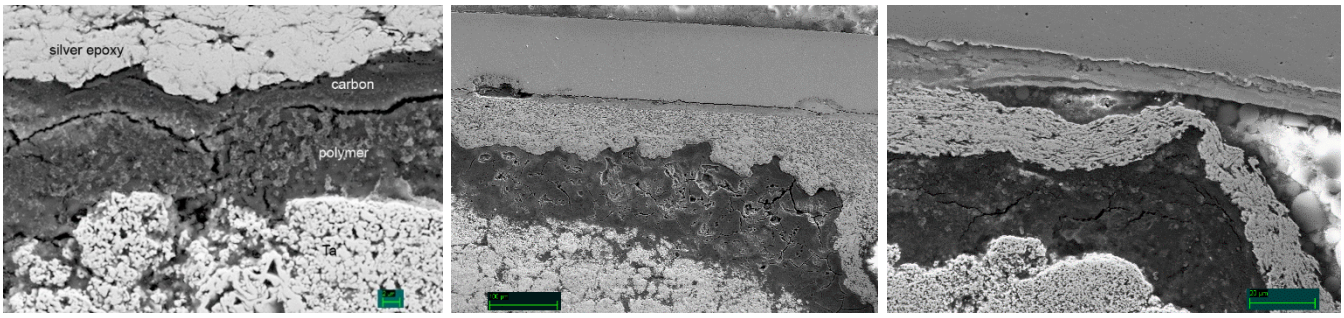

a) b) c)

Fig. 26. Cross-section of T530 capacitors after HTS at 150 ºC for 400 hr showing delamination and cracking between the silver epoxy and carbon and between carbon and polymer layers. (a) 150 µF SN17 failed ESR at 5.4 ohm; (c) 220 µF SN36 failed at 520 mohm; (c) 330 µF SN34 failed at 76 mohm.

SUMMARY

1. Temperature and voltage dependencies of leakage currents in polymer capacitors are consistent with the Schottky/Simmons models. Excessive leakage currents in low-voltage CPTCs compared to MnO2 and wet tantalum capacitors are due to a relatively low barrier height at the polymer/Ta2O5 interface, 0.3 eV < Φ_B < 0.4 eV. Respectively, the average activation energy for intrinsic leakage currents at rated voltages is even less, 0.17 ±0.05 eV.

2. Leakage currents in CPTCs are increasing with time of operation at temperatures from 85 ºC to 145 ºC and voltages close to the rated. Catastrophic failures of the parts were observed with time under bias at high voltages close to breakdown. The rate of current degradation increases with temperature and voltage exponentially. The voltage acceleration constant B is in the range from 13 to 18, and activation energy, E_a, for tested general purpose capacitors (T520, T525, and T530) is from 1.1 eV to 1.3eV. For automotive grade parts, T598, E_a is greater, ~1.65 eV. Parametric and catastrophic failures of CPTCs are due to two different mechanisms: migration of oxygen vacancies in Ta2O5 dielectric for parametric failures and time dependent dielectric breakdown (TDDB) for catastrophic failures.

3. Some CPTCs had unstable, erratically changing or spiking leakage currents. The probability of spiking is lot-dependent and increases with the level and duration of stress. This behavior is a specific feature of polymer capacitors caused by a less effective self-healing compared to MnO2 and wet tantalum capacitors. To reduce the noise level during applications, capacitors with excessive spiking should be screened out by monitored burning-in that is

recommended at 105 ºC, 1.1VR for 40 hours. Recommended life test conditions: monitoring currents at 105 ºC, VR for 2000 hours.

4. Standard MnO2 chip tantalum capacitors are more stable under high temperature storage conditions compared to polymer cathode tantalum capacitors. DF and ESR in CPTCs might degrade substantially even at 100 ºC after a few thousand hours in air, whereas characteristics of MnO2 capacitors remain unchanged even after storage at 150 ºC for more than 1000 hours.

5. Different lots of CPTCs have different susceptibility to degradation and failures at high temperatures. Contrary to general purpose, T520, T525 and T530 capacitors, automotive grade CPTCs had no degradation of AC characteristics during 2000 hours of HTS at 125 ºC. However, transient leakage currents increased substantially. More analysis is necessary to understand the mechanism of anomalous transients and their significance for applications.

6. Assessments of the median times to parametric failures of AC characteristics during storage at different temperatures showed that the activation energy of the degradation is in the range from 0.5 eV to 0.85 eV. Estimations have shown that some part types might fail in less than a year of storage at 85 ºC. Degradation and failures of ESR during HTS are likely caused by oxidative degradation of polymers resulting in increasing of their electrical resistivity, cracking, and formation of delaminations. Decreasing of capacitance is due to increased ESR that reduces the roll-off frequency substantially. Degradation of DF might be caused by increased ESR and/or absorption losses due to generation of electron traps at the polymer/Ta2O5 interface.

7. Cross-sectioning analysis have shown that oxygen penetrates inside the package along the interfaces between the molding compound and lead frame and through the cracks in the package. This indicates the need for a reliable encapsulation of capacitors to assure their long-term performance at high temperatures. Cracking of the case that for MnO2 capacitors is considered mostly as a cosmetic defect that does not affect reliability of the parts, is much more detrimental for polymer capacitors. To assure long-term operation of CPTCs, each lot should pass HTS testing at 125 ºC for 1000 hrs and part types should be qualified by HTS at 100 ºC for 10,000 hours.

8. No degradation of AC and DC characteristics was observed during vacuum testing of CPTCs at 100 ºC for 1900 hours, whereas capacitors stored at 100 ºC in air increased ESR substantially. This indicates that desorption of moisture from polymers does not worsen the performance of capacitors and confirms the thermo-oxidative nature of the degradation. A substantial reduction of the degradation processes in vacuum improves stability of AC characteristics and increases operating and storage temperatures for the parts. However, self-healing capabilities of the capacitors in vacuum might be reduced compared to the operation in air. This requires more thorough screening and qualification procedures to eliminate parts and lots with excessive spiking for capacitors intended for space operations.

ACKNOWLEDGMENT

This work was sponsored by the NASA Electronic Parts and Packaging (NEPP) program. The author is thankful to Michael Sampson, NEPP Program Manager, for support of this investigation, Bruce Meinhold, ASRC Federal Space and Defense, Group Lead, for a review and discussions.

REFERENCES

[1] J. D. Prymak, P. Staubli, and M. Prevallet, "Derating review of Ta-MnO2 vs. Ta-polymer vs.Al-polymer vs. NbO-MnO2," presented at the CARTS Europe, Nice, Fr, 2004.
[2] J. Lewis. (2013). *Considerations for Polymer Capacitors in Extreme Environments*. Available: www.kemet.com/ExtremePolymerPaper
[3] S. Zedníček, J.Petržílek, P.Vanšura, M.Weaver, and C.Reynolds. (2015, Conductive Polymer Capacitors. Basic Guidelines. *AVX Technical information*. Available: http://www.avx.com/docs/techinfo/PolymerGuidelines.pdf
[4] M. Cozzolino, "Evaluation of Polymer Counter-Electrode Tantalum Capacitors for High Reliability Airborne Applications," in *CARTS International*, Las Vegas, NV, 2012, pp. 13-22.
[5] J. Young, "Polymer Tantalum Capacitors for Automotive Applications," in *CARTS International*, Santa Clara, CA, 2014, pp. 297-311.
[6] Wikipedia. (2015). *Polymer capacitor*. Available: https://en.wikipedia.org/wiki/Polymer_capacitor
[7] J. Young, "High Voltage Polymer Aluminum and Tantalum Capacitors," presented at the APEC Applied Power Electronics Conference, 2013.
[8] J. Petrzilek, M. Biler, and T. Zednicek, "Hermetically Sealed Conductive Polymer Tantalum Capacitors," in *CARTS International*, Santa Clara, CA, 2014, pp. 287-292.
[9] Y. Freeman, G. F. Alapatt, W. R. Harrell, I. Luzinov, P. Lessner, and J. Qazi, "Anomalous Currents in Low Voltage Polymer Tantalum Capacitors," *Ecs Journal of Solid State Science and Technology*, vol. 2, pp. N197-N204, 2013.
[10] J. Lewis. (2013, November). *Introduction to polymer capacitors*. Available: http://www.electronicproducts.com/Passive_Components/Capacitors/Introduction_to_polymer_capacitors.aspx

[11] Y. Freeman, P. Lessner, E. Jones, H. Bishop, J. Pedroso, H. Perkins, *et al.*, "Hermetically Sealed Polymer Tantalum Capacitors and High Reliability," presented at the ESA 1st International Symposium 'Space Passive Component Days', Noordwijk, The Netherlands, 2013.
[12] A. Teverovsky, "Analysis of Weibull Grading Test for Solid Tantalum Capacitors," in *CARTS Europe*, Munich, Ge, 2010, pp. 103-120.
[13] E. Reed and C. Caetano, "New Reliability Assessment Practices for Tantalum Polymer Capacitors," presented at the ESA 1st International Symposium 'Space Passive Component Days', Noordwijk, The Netherlands, 2013.
[14] K. Norrman, M. V. Madsen, S. A. Gevorgyan, and F. C. Krebs, "Degradation Patterns in Water and Oxygen of an Inverted Polymer Solar Cell," *Journal of the American Chemical Society*, vol. 132, pp. 16883-16892, Dec 2010.
[15] K. Kawano, R. Pacios, D. Poplavskyy, J. Nelson, D. D. C. Bradley, and J. R. Durrant, "Degradation of organic solar cells due to air exposure," *Solar Energy Materials and Solar Cells*, vol. 90, pp. 3520-3530, 2006.
[16] S. H. Y. Freeman, P.Lessner, J.Chan, T.Kinard, E.Jones, H.Bishop, "Advancee in polymer hermetic seal (PHS) tantalum capacitors," presented at the Quality and Reliability Technical Symposium (QRTS) Hilton Phoenix/Mesa, 2015.
[17] A. Teverovsky, "Evaluation of Polymer Hermetically Sealed Tantalum Capacitors," NASA/GSFC, Greenbelt, MD2014.
[18] A. Teverovsky, "Leakage currents and gas generation in advanced wet tantalum capacitors," NASA/GSFC, Greenbelt, MD2015.
[19] A. Teverovsky, "Insulation Resistance and Leakage Currents in Low-Voltage Ceramic Capacitors With Cracks," *Components, Packaging and Manufacturing Technology, IEEE Transactions on*, vol. 4, pp. 1169-1176, 2014.
[20] J. G. Simmons, "Richardson-Schottky effect in solids," *Physical Review Letters*, vol. 15, pp. 967-968, 1965.
[21] T. J. Bright, J. I. Watjen, Z. M. Zhang, C. Muratore, A. A. Voevodin, D. I. Koukis, *et al.*, "Infrared optical properties of amorphous and nanocrystalline Ta2O5 thin films," *Journal of Applied Physics*, vol. 114, p. 083515, 2013.
[22] A. Teverovsky, "Leakage Currents in Low-Voltage PME and BME Ceramic Capacitors," presented at the 7th International Conference on Electroceramics (ICE2015), Penn Stater Conference Center, State College PA, USA, 2015.
[23] A. Teverovsky, "Degradation of leakage currents and reliability prediction for tantalum capacitors," in *2016 Annual Reliability and Maintainability Symposium (RAMS)*, 2016, pp. 1-7.
[24] J. L. Paulsen, E. K. Reed, and J. N. Kelly, "Reliability of Tantalum Polymer Capacitors," in *CARTS 2004: 24th Annual Capacitor and Resistor Technology Symposium*, 2004, pp. 114-121.
[25] E. K. Reed, J. N. Kelly, and J. L. Paulsen, "Reliability of Low-Voltage Tantalum Polymer Capacitors," in *CARTS USA 2005*, Palm Springs, CA, 2005, pp. 189-198.
[26] E. Reed and G. Haddox, "Reliability of High-Voltage Tantalum Polymer Capacitors," in *CARTS International*, Jacksonville, FL, 2011, p. 3.3.
[27] A. Teverovsky, "Scintillation Breakdowns and Reliability of Solid Tantalum Capacitors," *IEEE Transactions on device and materials reliability*, vol. 9, pp. 318-324, 2009.
[28] J. W. McPherson, *Reliability Physics and Engineering: Time-To-Failure Modeling*: Springer, 2013.
[29] Y. Jin, Q. Chen, and P. Lessner, "Thermal Stability Investigation of PEDOT Films from Chemical Oxidation and Prepolymerized Dispersion," *Electrochemistry*, vol. 81, pp. 801-803, 2013.
[30] J. Huang, P. F. Miller, J. C. de Mello, A. J. de Mello, and D. D. C. Bradley, "Influence of thermal treatment on the conductivity and morphology of PEDOT/PSS films," *Synthetic Metals*, vol. 139, pp. 569-572, 10/9/ 2003.
[31] P. M. J. Huang, J. Wilson, A. Mello, J. Mello, D. Bradley, "Investigation of the Effects of Doping and Post-Deposition Treatments on the Conductivity, Morphology, and Work Function of Poly(3,4-ethylenedioxythiophene)/Poly(styrene sulfonate) Films," *Advanced functional materials*, vol. 15, pp. 290-296, 2005.
[32] P. Gijsman, "Review on the thermo-oxidative degradation of polymers during processing and in service," in *e-Polymers* vol. 8, ed, 2008, p. 727.
[33] J. D. Peterson, S. Vyazovkin, and C. A. Wight, "Kinetics of the Thermal and Thermo-Oxidative Degradation of Polystyrene, Polyethylene and Poly(propylene)," *Macromolecular Chemistry and Physics*, vol. 202, pp. 775-784, 2001.
[34] J. L. Autran, P. Paillet, J. L. Leray, and R. A. B. Devine, "Conduction properties of amorphous Ta205 films prepared by plasma enhanced chemical vapour deposition," *Sensors and Actuators*, vol. A51, pp. 5-8, 1995.
[35] C. Chaneliere, J. Autran, R. Devine, and B. Balland, "Tantalum pentoxide (Ta2O5) thin films for advanced dielectric applications," *Material Science and Engineering*, vol. R22, pp. 269-322, 1998.
[36] A. Teverovsky, "Effect of Preconditioning and Soldering on Failures of Chip Tantalum Capacitors," NASA/GSFC, Greenbelt, MD 2014.